Clays and Clay Minerals, Vol. 67, No. 1:91–98, 2019

CYTOTOXICITY AND BIOKINETIC EVALUATION OF CLAY MINERALS

Soo-Jin Choi[1] *

[1]Division of Applied Food System, Major of Food Science & Technology, Seoul Women's University, Hwarang-ro 621, Nowon-gu, Seoul 01797, Republic of Korea

Abstract—Clay minerals, such as layered double hydroxide (LDH) and montmorillonite (MMT), have attracted a great deal of attention for biological applications. Along with the rapid development of nanotechnology, public concern about the potential toxicity of nanoparticles is growing. In the present work, cytotoxicity of LDH and MMT was assessed in terms of inhibition of cell proliferation, generation of oxidative stress, and induction of inflammation response. Moreover, the biokinetics of LDH and MMT were evaluated; biokinetics provides information about in vivo absorption, distribution, and excretion kinetics. The results demonstrated that both LDH and MMT inhibited cell proliferation at relatively large concentrations and after long exposure time compared to other inorganic nanoparticles, although they generated reactive oxygen species (ROS). LDH induced pro-inflammatory cytokines in a size-dependent manner. Biokinetic study revealed that, after single-dose oral administration to mice, both LDH and MMT had extremely slow oral rates of absorption and did not accumulate in any specific organ. All the results suggest great potential of clay minerals for biological application at safe levels.

Keywords—Absorption · Distribution · Excretion · Inflammation · Layered double hydroxide · Montmorillonite · Oxidative stress

CLAY MINERALS

For a long time, interest has been focused on clay minerals because they are abundant in nature and have potential for various applications. Clay minerals have a large surface area to volume ratio, ion exchange capacity, adsorption ability, and mucoadhesive property, which are fascinating as drug delivery carriers (Choy et al., 2007). In particular, layered double hydroxide (LDH), so-called anionic clay, consists of positively charged metal hydroxide sheets and interlayers of charge-compensating anions hydrated with water molecules. Recently, LDHs have been exploited extensively as delivery carriers for medical and biological purposes (Choi & Choy, 2011a, 2011b; Choi et al., 2008a, 2010). A class of cationic clays, montmorillonite (MMT), is a bio-inspired layered material and applied widely for pharmaceutical formulation (Baek & Choi, 2012; Baek et al., 2012a). Although LDH and MMT are accepted generally as low-toxic materials, little information is actually available about their in vitro and in vivo toxicity.

EFFECT OF CLAY MINERALS ON CELL PROLIFERATION OR VIABILITY

The short-term effect of clay minerals on cell proliferation can be evaluated with 3-(4,5-dimethylthiazol-2-yl)-2,5-diphenyltetrazolium bromide (MTT) or water soluble tetrazolium salt-1 (WST-1) assay after 24–72 h exposure. These are colorimetric assays, which measure the reduction of MTT or WST-1 by mitochondrial dehydrogenase in viable cells, giving rise to purple or dark red formazan. As a result, the assays actually measure the net metabolic activity of cells, thereby being reflective of the number of viable cells.

LDH nanoparticles (NPs) of various sizes (50, 100, 200, and 350 nm) did not inhibit remarkably cell proliferation of lung epithelial A549 cells, except at high concentrations (250–500 μg/mL after 48 h) (Fig. 1a) (Choi et al., 2008b). However, the inhibition of cell proliferation by LDH-NPs (200 nm) was much less than that caused by iron oxide, silica, and single-walled carbon nanotube (SWCNT) (Fig. 1b) (Choi et al., 2009). MMT was also found to affect the proliferation of human intestinal INT-407 cells, but at a high concentration of >100 μg/mL after 48–72 h (Fig. 1c) (Baeket al., 2012b). Worth noting is that the cytotoxicity of LDH-NPs can be affected strongly by their physicochemical properties and chemical composition (Baek et al., 2011; Choi & Choy, 2011a, 2011b).

A soluble cytosolic enzyme, lactate dehydrogenase, present in eukaryotic cells, is released into the extracellular cell culture medium when the cell plasma membrane is damaged, thereby directly reflecting cell death. Thus, the released levels of lactate dehydrogenase by LDH-NPs were also evaluated. Size-dependent release of lactate dehydrogenase was found from A549 cells incubated with LDH-NPs for 48 h, showing that the greatest membrane damage was caused by 50 nm-sized NPs (Fig. 2a) (Choi et al., 2008b). Meanwhile, relatively low levels of enzyme release by LDH (200 nm) were found compared to those caused by iron oxide or silica (Fig. 2b) (Choi et al., 2009), which is in good agreement with the results obtained by MTT assay (Fig. 1b). On the other hand, MMT released significant levels of enzyme only at 1000 μg/mL after 48–72 h of exposure (Fig. 2c) (Baek et al., 2012b).

The long-term effect on cell proliferation can be investigated using clonogenic assay. This measures colony-forming ability, based on the fact that a single cell grows into a colony. Here, a colony is defined as a cluster of at least 50 cells, and a relatively long time exposure of 7–14 days depending on the cell line needed for colony formation. The colony can be determined after fixation with methanol and staining with crystal violet. MMT inhibited significant colony-formation ability after exposure for 10 days (Fig. 3) (Baek et al., 2012b). However, worth noting is that in vitro long-time exposure to NPs is meaningful only when the NPs are observed to accumulate in specific organs. This type of assay is applied widely to evaluate whether an anticancer drug or therapy can reduce clonogenic survival of tumor cells.

* E-mail address of corresponding author: sjchoi@swu.ac.kr
DOI: 10.1007/s42860-019-0007-y

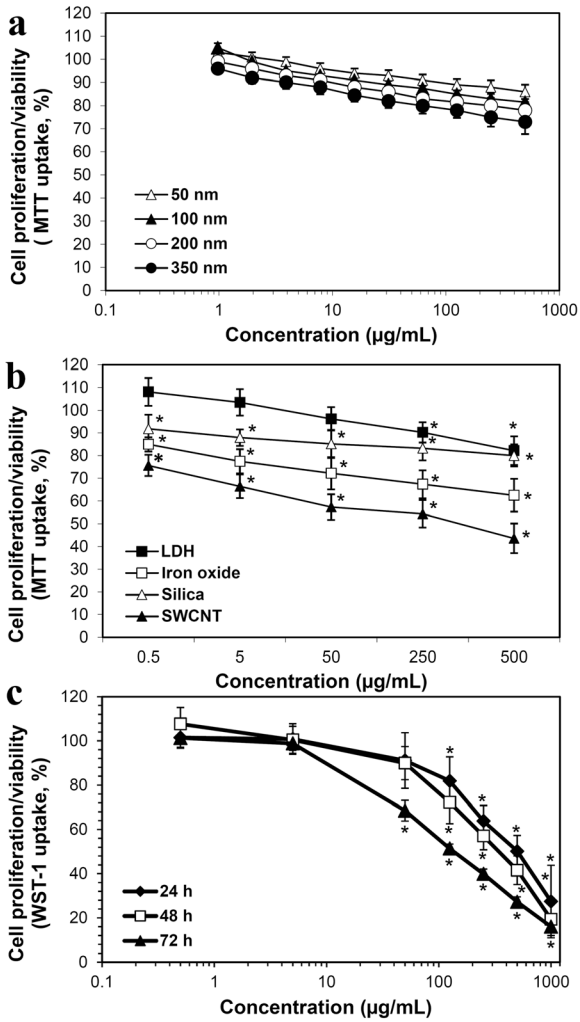

Fig. 1 Effect of LDH-NPs on cell proliferation of human lung epithelial A549 cells with respect to particle size after incubation for (**a**) 48 h and (**b**) concentration after incubation for 72 h. (**c**) Effect of MMT on human intestinal INT-407 cells with respect to concentration and incubation time. * denotes significant difference from the untreated control ($p < 0.05$). Reproduced, in part, from Choi et al. (2008b, 2009), and Baek et al. (2012b) with the permission of American Scientific Publishers, Elsevier, and Springer Nature, respectively

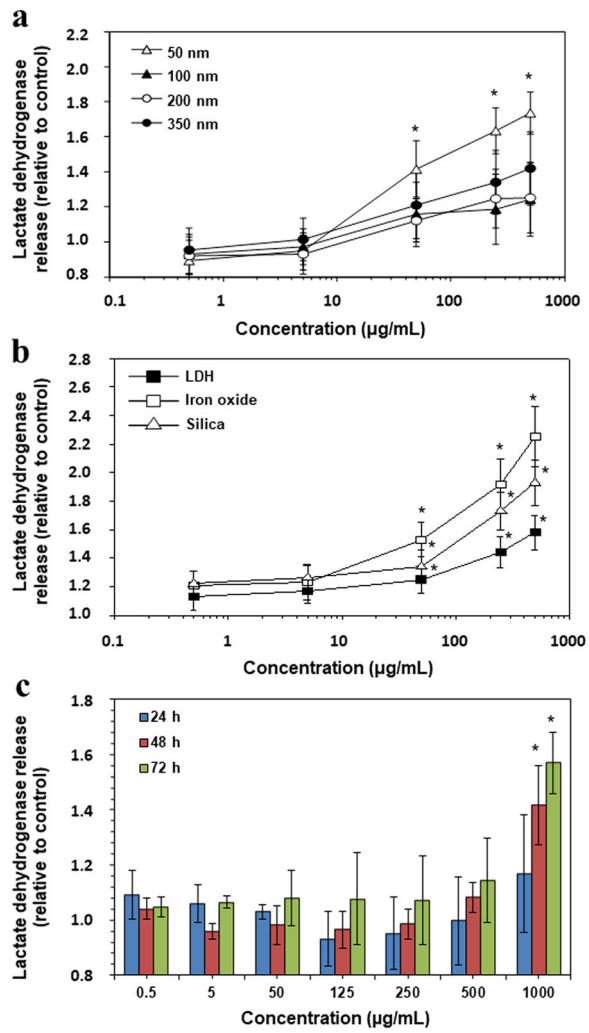

Fig. 2 Lactate dehydrogenase release from A549 cells treated with different sized LDH-NPs for (**a**) 48 h or (**b**) incubated with LDH, iron oxide, or silica for 72 h. (**c**) Released levels of lactate dehydrogenase from MMT-exposed INT-407 cells with respect to concentration and incubation time. * denotes significant difference from the untreated control ($p < 0.05$). Reproduced, in part, from Choi et al. (2008b, 2009) with the permission of American Scientific Publishers, Elsevier, and Springer Nature, respectively

EFFECT OF CLAY MINERALS ON OXIDATIVE STRESS

Several types of NPs were reported as causing oxidative stress; oxidative stress can be evaluated by measuring the levels of reactive oxygen species (ROS) inside cells. The cell-permeant 2′,7′-dichlorodihydrofluorescein diacetate (H_2DCFDA) dye is applied as an indicator of intracellular ROS. The dye is non-fluorescent, but converts to green fluorescent dichlorofluorescein (DCF) upon oxidation by ROS after cleavage by intracellular esterases.

LDH-NPs (200 nm) and MMT were found to generate ROS (Fig. 4a and b) in A549 cells and INT-407 cells, respectively, indicating induction of oxidative stress (Baek et al., 2012; Choi et al., 2009). However, ROS generation was observed only at high concentration (>100 μg/mL) and after 48–72 h exposure. Moreover, relatively low ROS generation by LDH-NPs was observed compared to SWCNT.

Oxidative stress caused by NPs was further evaluated by analyzing antioxidant enzymes, such as catalase (CAT), glutathione reductase (GR), superoxide dismutase (SOD), and heme oxygenase-1 (HO-1), in LDHs-exposed A549 cells (Choi et al., 2015). These enzymes metabolize oxidative toxic intermediates, and their expression and activity increase the protection of cells against oxidative stress. The activity of CAT, GR, SOD, and HO-1 increased in cells exposed to LDH-NPs (100 nm) at 250–1000 μg/mL for 24 h (Fig. 4c) (Choi et al., 2015). But, the antioxidant enzyme activity increased rapidly

https://doi.org/10.1007/s42860-019-0007-y Published online by Cambridge University Press

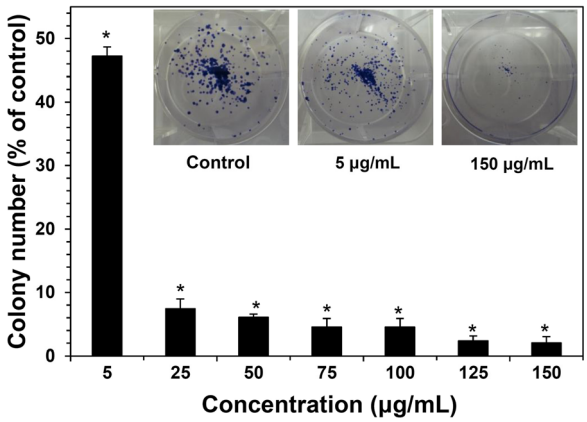

Fig. 3 Long-term inhibition of colony formation caused by MMT after exposure for 10 days. * denotes significant difference from the untreated control ($p < 0.05$). Reproduced, in part, from Baek et al. (2012b) with the permission of Springer Nature

even after 1 h of exposure to 500 μg/mL LDH-NPs (Fig. 4d). Interestingly, LDH-NPs at a concentration of 500 μg/mL did not inhibit cell proliferation for 24 h (Choi et al., 2015). LDH-NPs are likely, therefore, to produce ROS, thereby increasing antioxidant enzyme activity in order to control and neutralize ROS. The detoxification process by antioxidant enzymes may have a minor effect on cell proliferation (Fig. 1b).

Indeed, diverse NPs including CNT, silica, iron oxide, and zinc oxide (ZnO) have been reported to cause oxidative stress, but at much lower concentration levels and after shorter time exposure than LDH-NPs (Ng et al., 2017; Pongrac et al., 2016; Shvedova, Pietroiusti, Fadeel & Kagan, 2012; Zuo et al., 2016).

EFFECT OF CLAY MINERALS ON INFLAMMATION RESPONSE

Inflammation can be a toxicity endpoint caused by diverse types of NPs. In vitro inflammation induction is evaluated by measuring the levels of pro-inflammatory cytokines, such as interleukin-1 (IL-1), IL-6, IL-8, and tumor necrosis factor (TNF). Pro-inflammatory cytokines are signaling molecules, which are excreted from immune cells and other cell types that promote inflammation. These cytokines play a role in mediating the innate immune response.

LDH-NPs (200 nm) were determined to induce a pro-inflammatory cytokine, IL-8, from A549 cells at concentrations > 125 μg/mL in a time-dependent manner (Fig. 5a) (Choi et al., 2009). The highest level of IL-8 was induced by 50 nm particles, compared to 100, 200, and 350-nm particles (Fig. 5b), indicating the inflammation potential caused by LDH-NPs (Choi et al., 2008b). On the other hand, of LDH-NPs (100 nm)-induced pro-inflammatory cytokines, only IL-6 and IL-8, but not IL-1 and TNF-α, resulted from oxidative stress (Choi et al., 2015). Silica and carbon nanotubes were also reported to have induced an inflammation response (Chan et al., 2018; Poulsen et al., 2016).

CELLULAR TRAFFICKING OF CLAY MINERALS

Most NPs are now well known to be taken up by cells via an energy-dependent endocytic pathway, such as clathrin-mediated

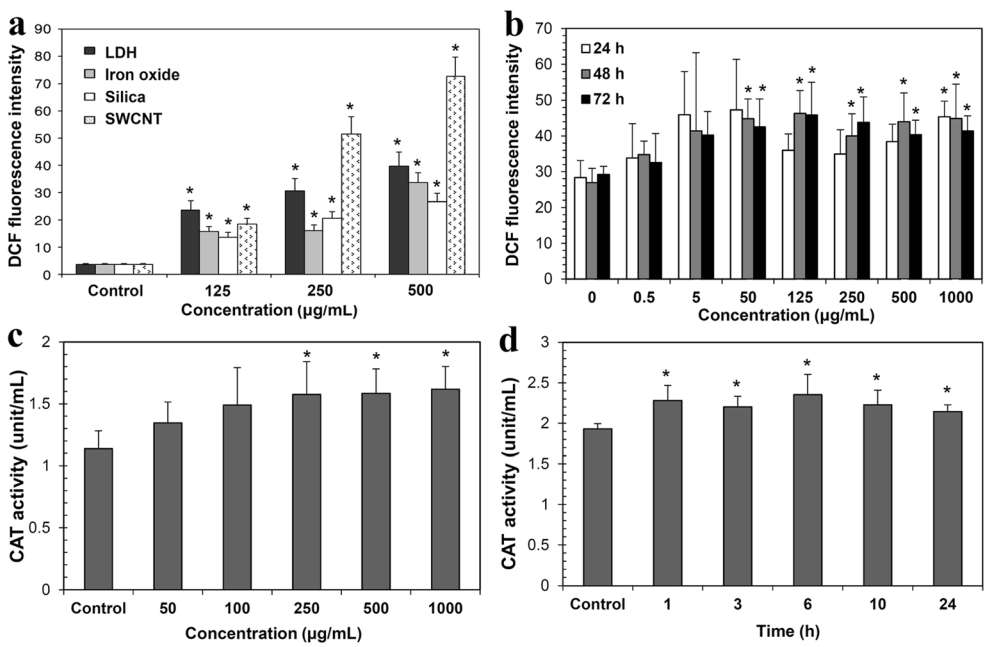

Fig. 4 ROS generation caused by (**a**) LDH, iron oxide, silica, and SWCNT after incubation for 72 h and by (**b**) MMT with respect to concentration and incubation time. Increased CAT activity (**c**) in LDH-NPs-treated A549 cells with respect to concentration after incubation for 24 h and (**d**) in 500 μg/mL LDH-treated cells with respect to incubation time. * denotes significant difference from the untreated control ($p < 0.05$). Reproduced, in part, from Choi et al. (2009, 2015) and Baek et al. (2012b) with the permission of Elsevier, Springer Nature, and Dovepress, respectively

https://doi.org/10.1007/s42860-019-0007-y Published online by Cambridge University Press

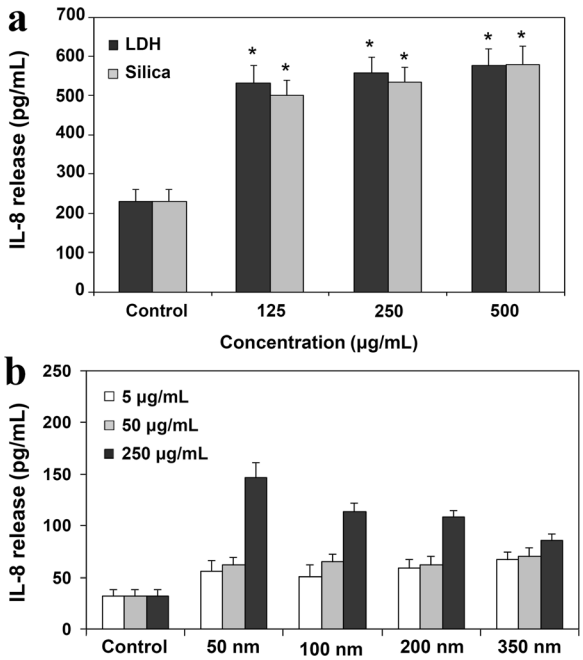

Fig. 5 Pro-inflammatory mediator, IL-8, release from A549 cells (**a**) treated with LDH or silica NPs for 72 h or (**b**) treated with different-sized LDH-NPs for 48 h. * denotes significant difference from the untreated control ($p < 0.05$). Reproduced, in part, from Choi et al. (2008b, 2009) with the permission of American Scientific Publisher and Elsevier, respectively

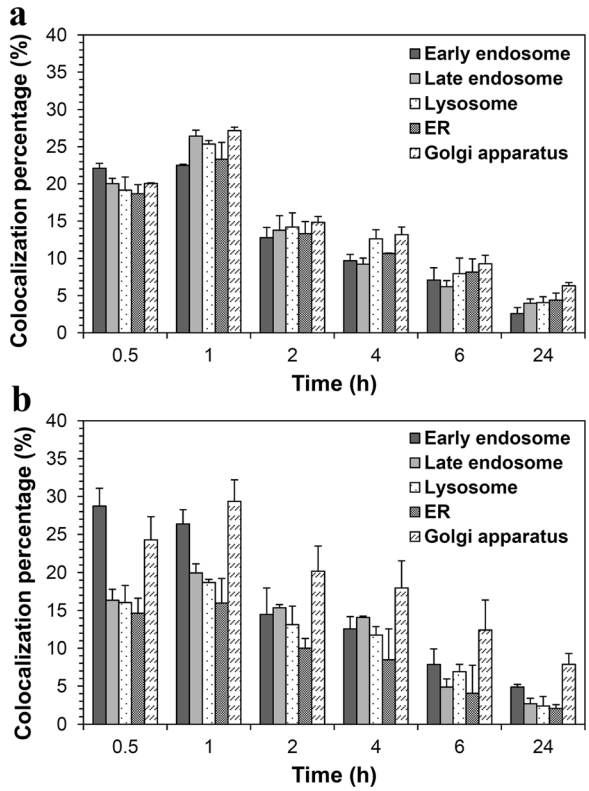

Fig. 6 Quantitative analysis of 50 nm (**a**) and 100 nm (**b**) LDH colocalization with intracellular organelles. Reproduced, in part, from Chung et al. (2012) with the permission of Elsevier

endocytosis (Oh et al., 2006, 2009). Understanding the fate and trafficking pathway of NPs after internalization into cells is important for predicting their potential toxicity and delivery efficiency. Transport of NPs from plasma membrane to endocytic organelles, such as endosomes, lysosome, the Golgi apparatus, the endoplasmic reticulum (ER), and nucleus can be evaluated using immunofluorescence assay, followed by quantification using confocal microscopy. Conjugation of NPs to a fluorescent dye, such as fluorescein 5′-isothiocyanate (FITC), is also necessary to determine the colocalization of NPs with specific organelles. Here, endosome is an intracellular membrane-bound compartment, transporting molecules from plasma membrane to lysosomes or recycling back from the Golgi. Lysosome is a type of vesicle, which can degrade diverse biomolecules with the help of hydrolytic enzymes and low pH (4.5–5.0). The ER plays a role in protein folding and molecule transport to the Golgi. The Golgi apparatus is a collection, packaging, and modifying step of proteins received from the ER for secretion via exocytosis. The cell nucleus contains most of the genetic materials, controlling gene expression.

The intracellular fate of LDH-NPs-FITC of two different sizes (50 and 100 nm) was investigated, showing different trafficking pathways depending on particle size (Fig. 6) (Chung et al. 2012). Smaller particles, 50 nm, follow both a typical early endosome-late endosome-lysosome endocytic pathway and an exocytic pathway represented by early endosome-the Golgi-the ER-the Golgi (Fig. 6a). Whereas, 100 nm particles escape a typical endo-lysosomal degradation and are found massively in the exocytic organelles, including the ER and the Golgi complex (Fig. 6b). Hence, 100 nm LDH-NPs can be effective delivery carriers for genes, which are easy to break down in lysosome. Both differently sized LDH-NPs were localized in early endosome as soon as 0.5 h post-treatment and were retained inside the cells for more than 24 h. In any case, LDH-NPs were not found in nuclei, implying they have low genotoxicity potential.

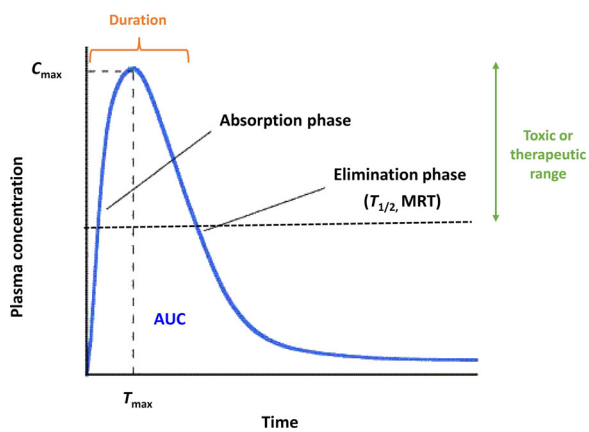

Fig. 7 Typical plasma concentration-time profile and biokinetic parameters of molecules following oral administration

https://doi.org/10.1007/s42860-019-0007-y Published online by Cambridge University Press

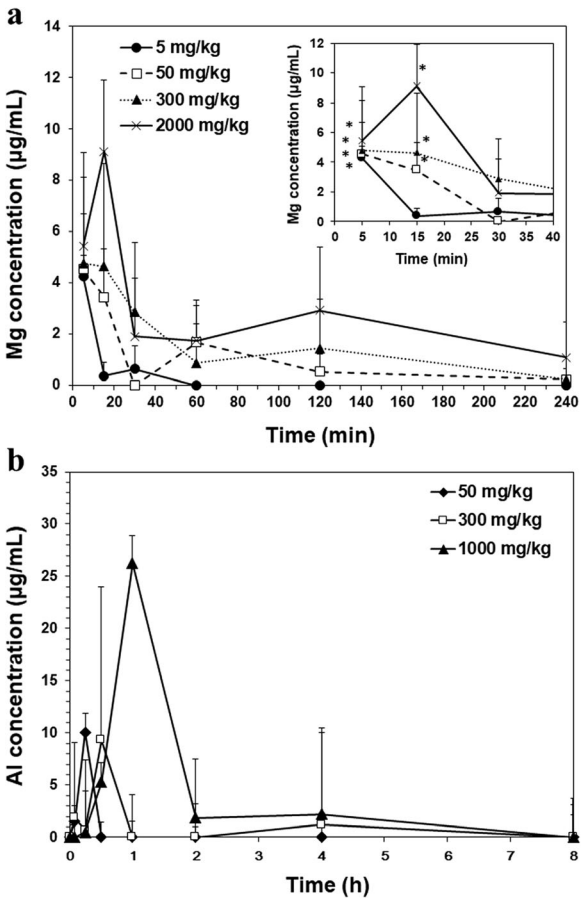

Fig. 8 Plasma concentration vs. time curves for LDH-NPs (**a**) and MMT (**b**) after single-dose oral administration to mice. * denotes significant difference from the untreated control ($p < 0.05$). Reproduced, in part, from Baek et al. (2011) and Yu et al. (2013) with the permission of Springer Nature and Hindawi, respectively

BIOKINETICS OF CLAY MINERALS

Absorption

Biokinetics is a term similar to pharmacokinetics for drugs or toxicokinetics for toxic materials, but it is used for materials the physiological activity of which has not been determined. Biokinetic study is a branch of pharmacology and the quantification of the time line of biomolecules in the body during the process of absorption, distribution, metabolism, and excretion or clearance. In other words, biokinetics is a reflection of how the body treats biomolecules, as indicated by the plasma concentration-time curves after administration. Biokinetic parameters can be obtained from the plasma concentration vs. time profiles (Fig. 7). For example, the area under the concentration-time curve (AUC) represents the total amount of a molecule that reaches the circulation system in a given time, representing absorption or bioavailability. Other parameters, such as maximum concentration (C_{max}), time for maximum concentration (T_{max}), half-life ($T_{1/2}$), and mean residence time (MRT) can be obtained, which are used to predict the absorption or elimination phases. On the other hand, absorption (%) can be calculated from the AUC value divided by total administered dose.

The biokinetics of LDH-NPs (100 nm) was evaluated after single-dose oral administration (5, 50, 300, and 2000 mg/kg) to mice (Fig. 8a) (Yu et al., 2013). At least two different doses are generally recommended if biokinetic behaviors are not well determined. The plasma concentration-time curves of LDH-NPs show that NPs rapidly entered the bloodstream even at the highest dose of 2000 mg/kg and were not retained in the systemic circulation for a long time (Fig. 8a), as indicated by small T_{max}, $T_{1/2}$, and MRT values (Table 1). Oral absorption of LDH-NPs was found to be extremely small, showing 2.85, 1.37, 0.40, and 0.14% for 5, 50, 300, and 2000 mg/kg, respectively. This result suggests that a small amount of orally

Table 2 Biokinetic parameters of MMT after single-dose oral administration to mice

	50 mg/kg	300 mg/kg	1000 mg/kg
C_{max} (μg/mL)	10.07	9.32	26.24
T_{max} (h)	0.25	0.50	1.00
AUC [(h) × (μg/mL)]	2.08	3.53	25.55
$T_{1/2}$ (h)	0.32	0.65	1.19
MRT(h)	0.37	0.79	2.06

Abbreviation: C_{max}, maximum concentration; T_{max}, time to maximum concentration; AUC, area under the plasma concentration-time curve; $T_{1/2}$, half-life; MRT, mean residence time. Includes data from Baek et al. (2012b) which are reproduced with the permission of Springer Nature

Table 1 Biokinetic parameters of different doses of LDH-NPs after single-dose oral administration to mice

	5 mg/kg	50 mg/kg	300 mg/kg	2000 mg/kg
C_{max} (μg/mL)	4.15 ± 1.41	4.44 ± 0.32	7.24 ± 0.70	9.36 ± 1.92
T_{max} (h)	0.08 ± 0.00	0.14 ± 0.10	0.17 ± 0.10	0.21 ± 0.08
AUC [(h) x (μg/mL)]	0.79 ± 0.29	4.00 ± 2.36	8.74 ± 4.05	11.96 ± 6.29
$T_{1/2}$ (h)	0.22 ± 0.20	0.73 ± 0.49	1.38 ± 0.67	1.86 ± 0.10
MRT (h)	0.35 ± 0.29	1.27 ± 0.82	2.15 ± 1.27	3.14 ± 0.57

Abbreviation: C_{max}, maximum concentration; T_{max}, time to maximum concentration; AUC, area under the plasma concentration-time curve; $T_{1/2}$, half-life; MRT, mean residence time. Includes data from Yu et al. (2013) which are reproduced with the permission of Hindawi

https://doi.org/10.1007/s42860-019-0007-y Published online by Cambridge University Press

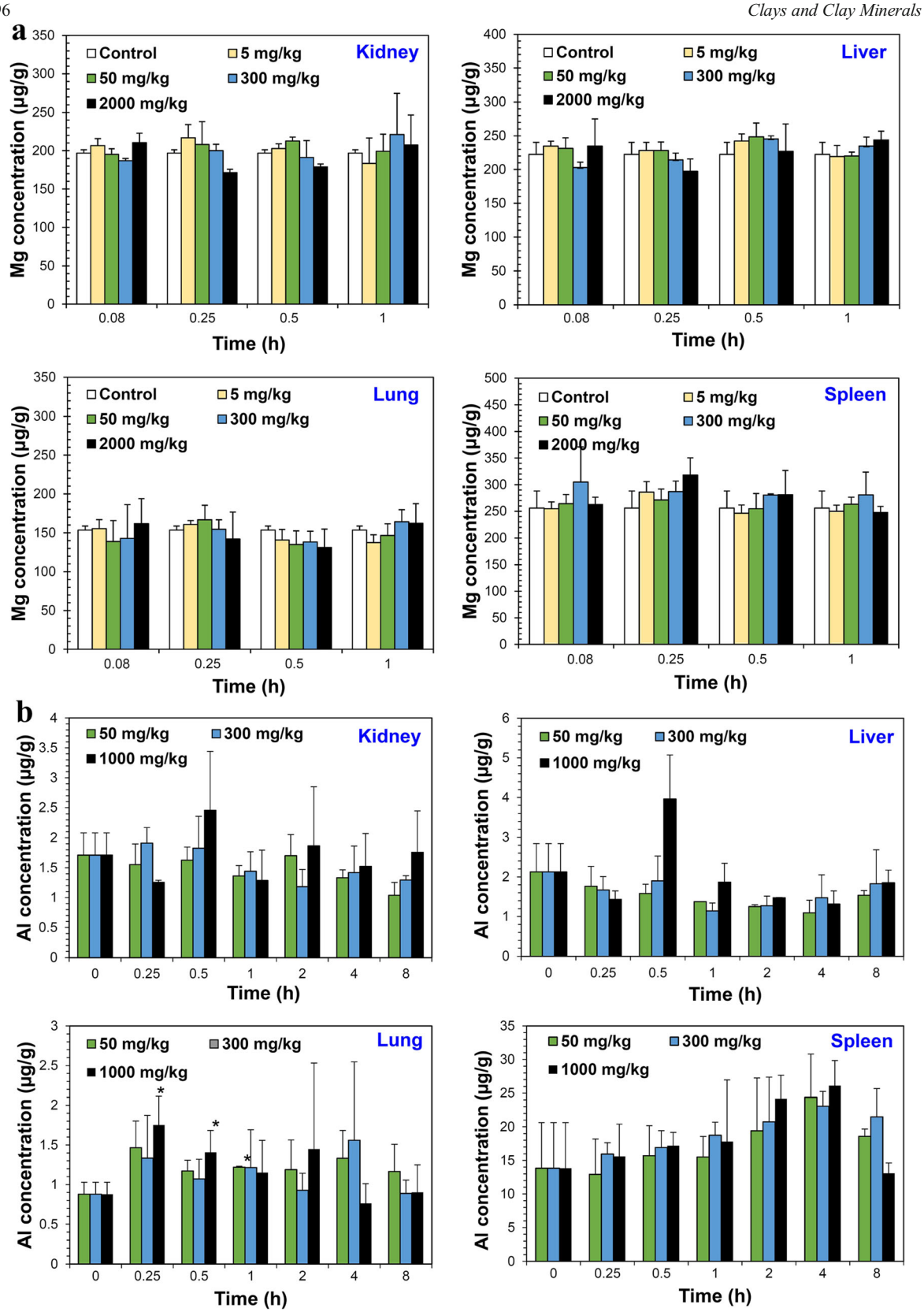

Fig. 9 Tissue distribution kinetics of LDH-NPs (**a**) and MMT (**b**) after single-dose oral administration to mice. * denotes significant difference from the untreated control ($p < 0.05$). Reproduced, in part, from Baek et al. (2012b) and Yu et al. (2013) with the permission of Springer Nature and Hindawi, respectively

https://doi.org/10.1007/s42860-019-0007-y Published online by Cambridge University Press

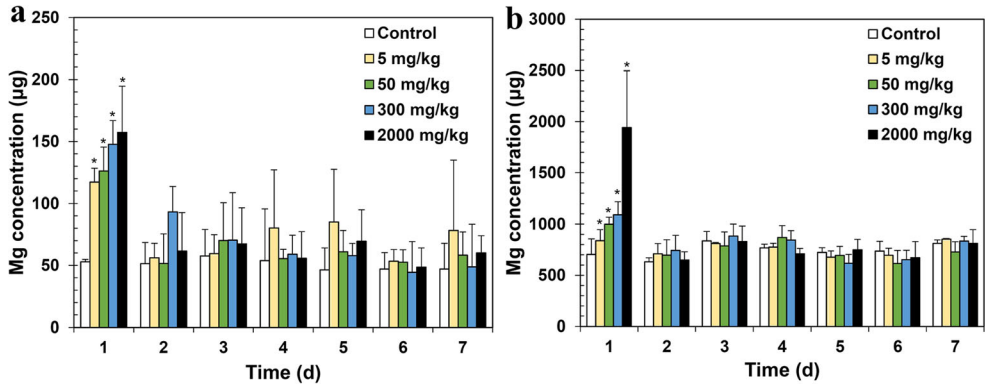

Fig. 10 Excretion kinetics of LDH-NPs via urine (**a**) and feces (**b**) after single-dose oral administration to mice. * denotes significant difference from the untreated control. Reproduced, in part, from Yu et al. (2013) with the permission of Hindawi

administered LDH-NPs can be absorbed and eliminated from the body within 4 h, implying their low toxicity potential.

On the other hand, when a biokinetic study of MMT (50, 300, and 1000 mg/kg) was performed following single-dose oral administration to mice, similar plasma concentration-time profiles to those for LDH-NPs were obtained (Fig. 8b) (Baek et al., 2012b). The peak concentrations of 50, 300, and 1000 mg/kg MMT reached at 0.25, 0.5, and 1 h post-oral administration and were retained in the body for 0.37, 0.79, and 2.06 h, respectively, as indicated by T_{max} and MRT values (Table 2). Exact oral absorption could not be calculated, because the uncertainty of the molecular weight of the MMT formula ($Na_{0.33}Al_2Si_4O_{10}(OH)_2{\cdot}nH_2O$) used.

Relatively little information about biokinetics or toxicokinetics of NPs is available. Oral absorption of ZnO-NPs of two different sizes (20 and 70 nm) was 10–30% depending on the dose administered (50, 300, and 2000 mg/kg), particle size (20 and 70 nm), and surface charge modification (positive and negative) (Baek et al., 2012c; Choi & Choy, 2014; Paek et al., 2013). A total of 6–12% of colloidal silica NPs entered the bloodstream following oral administration to rats, depending on dose (500, 1000, and 2000 mg/kg) and particle size (20 and 100 nm) (Paek et al., 2014). Although extremely small oral absorption (0.01–0.78% depending on dispersants used) of titanium dioxide (TiO_2) was reported recently (Jo et al., 2016; Kim et al., 2016), clearly the absorption of LDH-NPs is low compared to other inorganic NPs.

Table 3 Amount of LDH-NPs excreted via urine and feces after single-dose oral administration to mice

	5 mg/kg	50 mg/kg	300 mg/kg	2000 mg/kg
Excretion via urine (%)	3.33	2.4	1.3	0.28
Excretion via feces (%)	95.47	96.89	84.38	72.62

Includes data from Yu et al. (2013) which are reproduced with the permission of Hindawi

Tissue Distribution

Tissue distribution kinetics can be investigated after single-dose oral administration and sampling of organs, such as kidneys, liver, lungs, and spleen at several time points. Figure 9a shows that LDH-NPs (100 nm) did not accumulate in any specific organ, even at the highest dose of 2000 mg/kg (Yu et al., 2013). Significantly increased MMT levels were not found in kidneys, liver, or spleen, but were found in the in the lungs at 0.25–1 h post-oral administration (Baek et al., 2012b). Taken together, orally administered LDH-NPs and MMT did not accumulate in the body, suggesting their low toxicity.

Also worth noting here is that quantitative analysis of LDH or MMT in plasma or organ samples was performed by measuring total Mg or Al levels using inductively coupled plasma-optical emission spectroscopy (ICP-OES). Optimization of the pre-treatment method is necessary for complete digestion of organic materials with nitric acid, hydrogen peroxide, or other solvents. Moreover, because basal mineral levels can be detected in plasma or organ samples, the data should be presented as increases in Mg or Al levels in treated groups by subtracting basal Mg or Al levels in untreated controls after statistical analysis.

Excretion

Excretion kinetics can be evaluated using metabolic cages that enable urine and feces to be collected at several time points after single-dose administration (Yu et al., 2013). Figure 10 demonstrates that LDH-NPs (100 nm) were excreted from the body within 24 h via both urine and feces. When excretion amounts were calculated (Table 3), extremely small amounts of LDH-NPs were eliminated by urinary excretion, while most NPs were not absorbed, but excreted directly from the body via the fecal or biliary routes. Note that absorption amounts of LDH-NPs were very consistent with excretion amounts via urine. Orally absorbed LDH-NPs are very likely to be metabolized in organs and excreted via urine.

ACKNOWLEDGMENTS

This work was supported by the National Research Foundation of Korea (NRF) grant funded by the Korea government (MSIT) (No. 2018R1A2B6001238).

https://doi.org/10.1007/s42860-019-0007-y Published online by Cambridge University Press

REFERENCES

Baek, M. & Choi, S. J. (2012). Effect of orally administered glutathione-montmorillonite hybrid systems on tissue distribution. *Journal of Nanomaterials,* 2012, 469372.

Baek, M., Kim, I. S., Yu, J., Chung, H. E., Choy, J. H., & Choi, S. J. (2011). Effect of different forms of anionic nanoclays on cytotoxicity. *Journal of Nanoscience Nanotechnology,* 11, 1803–1806.

Baek, M., Choy, J. H., & Choi, S. J. (2012a). Montmorillonite intercalated with glutathione for antioxidant delivery: synthesis, characterization, and bioavailability evaluation. *International Journal of Pharmaceutics,* 425, 29–34.

Baek, M., Chung, H. E., Yu, J., Lee, J. A., Kim, T. H., Oh, J. M., Lee, W. J., Paek, S. M., Lee, J. K., Jeong, J., Choy, J. H., & Choi, S. J. (2012b). Pharmacokinetics, tissue distribution, and excretion of zinc oxide nanoparticles. *International Journal Nanomedicine,* 7, 3081–3097.

Baek, M., Lee, J. A., & Choi, S. J. (2012c). Toxicological effects of a cationic clay, montmorillonite in vitro and in vivo. *Molecular & Cellular Toxicology,* 8, 95–101.

Chan, J. Y. W., Tsui, J. C. C., Law, P. T. W., So, W. K. W., Leung, D. Y. P., Sham, M. M. K., Tsui, S. K. W., & Chan, C. W. H. (2018). RNA-Seq revealed ATF3-regulated inflammation induced by silica. *Toxicology,* 393, 34–41.

Choi, S. J., Choi, G. E., Oh, J. M., Oh, Y. J., Park, M. C., & Choy, J. H. (2010). Anticancer drug encapsulated in inorganic lattice can overcome drug resistance. *Journal of Materials Chemistry,* 20, 9463–9469.

Choi, S. J. & Choy, J. H. (2011a). Layered double hydroxide nanoparticles as target-specific delivery carriers: uptake mechanism and toxicity. *Nanomedicine,* 6, 803–814.

Choi, S. J. & Choy, J. H. (2011b). Effect of physico-chemical parameters on the toxicity of inorganic nanoparticles. *Journal of Materials Chemistry,* 21, 5547–5554.

Choi, S. J. & Choy, J. H. (2014). Biokinetics of zinc oxide nanoparticles: toxicokinetics, biological fates, and protein interaction. *International Journal of Nanomedicine,* 9, 261–269.

Choi, S. J. Oh, J. M., & Choy, J. H. (2008a). Human-related application and nanotoxicology of inorganic particles: complementary aspects. *Journal of Materials Chemistry,* 18, 615–620.

Choi, S. J., Oh, J. M., & Choy, J. H. (2008b). Safety aspect of inorganic layered nanoparticles: size-dependency in vitro and in vivo. *Journal of Nanoscience Nanotechnology,* 8, 5297–5301.

Choi, S. J., Oh, J. M., & Choy, J. H. (2009). Toxicological effects of inorganic nanoparticles on human lung cancer A549 cells. *Journal of Inorganic Biochemistry,* 103, 463–471.

Choi, S. J., Paek, H. J., & Yu, J. (2015). Oxidative stress by layered double hydroxide nanoparticles via an SFK-JNK and p38-NF-kappaB signaling pathway mediates induction of interleukin-6 and interleukin-8 in human lung epithelial cells. *International Journal of Nanomedicine,* 10, 3217–3229.

Choy, J. H., Choi, S. J., Oh, J. M., & Park, T. (2007). Clay minerals and layered double hydroxides for novel biological applications. *Applied Clay Science,* 36, 122–132.

Chung, H. E., Park, D. H., Choy, J. H., & Choi, S. J. (2012). Intracellular trafficking pathway of layered double hydroxide nanoparticles in human cells: Size-dependent cellular delivery. *Applied Clay Science,* 65–66, 24–30.

Jo, M. R., Yu, J., Kim, H. J., Song, J. H., Kim, K. M., Oh, J. M., & Choi, S. J. (2016). Titanium dioxide nanoparticle-biomolecule interactions influence oral absorption. *Nanomaterials (Basel),* 6.

Kim, M. K., Lee, J. A., Jo, M. R., & Choi, S. J. (2016). Bioavailability of silica, titanium dioxide, and zinc oxide nanoparticles in rats. *Journal of Nanoscience and Nanotechnology,* 16, 6580–6586.

Ng, C. T., Yong, L. Q., Hande, M. P., Ong, C. N., Yu, L. E., Bay, B. H., & Baeg, G. H. (2017). Zinc oxide nanoparticles exhibit cytotoxicity and genotoxicity through oxidative stress responses in human lung fibroblasts and Drosophila melanogaster. *International Journal of Nanomedicine,* 12, 1621–1637.

Oh, J. M., Choi, S. J., Kim, S. T., & Choy, J. H. (2006). Cellular uptake mechanism of an inorganic nanovehicle and its drug conjugates: Enhanced efficacy due to clathrin-mediated endocytosis. *Bioconjugugate Chemistry,* 17, 1411–1417.

Oh, J. M., Choi, S. J., Lee, G. E., Kim, J. E., & Choy, J. H. (2009). Inorganic metal hydroxide nanoparticles for targeted cellular uptake through clathrin-mediated endocytosis. *Chemistry – An Asian Journal,* 4, 67–73.

Paek, H. J., Chung, H. E., Lee, J. A., Kim, M. K., Lee, Y. J., Kim, M. S., Kim, S. H., Maeng, E. H., Lee, J. K., Jeong, J., & Choi, S. J. (2014). Quantitative determination of silica nanoparticles in biological matrices and their pharmacokinetics and toxicokinetics in rats. *Science of Advanced Materials,* 6, 1605–1610.

Paek, H. J., Lee, Y. J., Chung, H. E., Yoo, N. H., Lee, J. A., Kim, M. K., Lee, J. K., Jeong, J., & Choi, S. J. (2013). Modulation of the pharmacokinetics of zinc oxide nanoparticles and their fates in vivo. *Nanoscale,* 5, 11416–11427.

Pongrac, I. M., Pavicic, I., Milic, M., Brkic Ahmed, L., Babic, M., Horak, D., Vinkovic Vrcek, I., & Gajovic, S. (2016). Oxidative stress response in neural stem cells exposed to different superparamagnetic iron oxide nanoparticles. *International Journal of Nanomedicine,* 11, 1701–1715.

Poulsen, S. S., Jackson, P., Kling, K., Knudsen, K. B., Skaug, V., Kyjovska, Z. O., Thomsen, B. L., Clausen, P. A., Atluri, R., Berthing, T., Bengtson, S., Wolff, H., Jensen, K. A., Wallin, H., & Vogel, U. (2016). Multi-walled carbon nanotube physicochemical properties predict pulmonary inflammation and genotoxicity. *Nanotoxicology,* 10, 1263–1275.

Shvedova, A. A., Pietroiusti, A., Fadeel, B., & Kagan, V. E. (2012). Mechanisms of carbon nanotube-induced toxicity: focus on oxidative stress. *Toxicology and Applied Pharmacology,* 261, 121–133.

Yu, J., Chung, H. E., & Choi, S. J. (2013). Acute oral toxicity and kinetic behaviors of inorganic layered nanoparticles. *Journal of Nanomaterials.* https://doi.org/10.1155/2013/628381.

Zuo, D., Duan, Z., Jia, Y., Chu, T., He, Q., Yuan, J., Dai, W., Li, Z., Xing, L., & Wu, Y. (2016). Amphipathic silica nanoparticles induce cytotoxicity through oxidative stress mediated and p53 dependent apoptosis pathway in human liver cell line HL-7702 and rat liver cell line BRL-3A. *Colloids and Surfaces B: Biointerfaces,* 145, 232–240.

(*Received 25 April 2018; revised 7 August 2018; AE: J.-H. Choy*)